

High- p_{\perp} charged-pion production in Pb-Au Collisions at 158 AGeV/c

G. Agakichiev^a, R. Baur^b, P. Braun-Munzinger^c, A. Drees^d, S. Esumi^b,
 U. Faschingbauer^{b,e}, Z. Fraenkel^f, Ch. Fuchs^e, P. Glässel^b, C.P. de los Heros^f, P. Holl^g,
 Ch. Jung^b, B. Lenkeit^b, F. Messer^{d*}, M. Messer^b, Y. Panebrattsev^a, A. Pfeiffer^b, J. Rak^e,
 I. Ravinovich^f, S. Razin^a, P. Rehak^g, M. Richter^b, N. Saveljic^a, J. Schukraft^h,
 S. Shimansky^a, W. Seipp^b, E. Socol^f, H.J. Specht^b, J. Stachel^b, G. Tel-Zur^f,
 I. Tserruya^f, T. Ullrich^b, C. Voigt^b, C. Weber^b, J.P. Wessels^b, T. Wienold^b, J.P. Wurm^e,
 V. Yurevich^a

* F. Messer: Doctoral Thesis of Federica Ceretto, University of Heidelberg (1998);

^a JINR, Dubna, Russia; ^b Universität Heidelberg, Germany; ^c GSI, Darmstadt, Germany; ^d State University of New York at Stony Brook, USA ^e Max-Planck-Institut für Kernphysik, Heidelberg, Germany; ^f Weizmann Institute of Science, Rehovot, Israel; ^g Brookhaven National Laboratory, Upton, USA; ^h CERN, Geneva, Switzerland;

The CERES/NA45 experiment at the CERN SPS measured transverse momentum spectra of charged-pions in the range $1 < p_{\perp} < 4$ GeV/c near mid-rapidity ($2.1 < y < 2.6$) in 158 AGeV/c Pb-Au collisions. The invariant transverse momentum spectra are exponential over the entire observed range. The average inverse slope is 245 ± 5 MeV/c, it shows a 2.4% increase with centrality of the collision over the 35% most central fraction of the cross section. The π^{-}/π^{+} ratio is constant at 1.028 ± 0.005 over the p_{\perp} interval measured.

Transverse momentum distributions of hadrons which emerge from particle collisions are closely related to the collision dynamics. In general, below 1 GeV/c the p_{\perp} spectra exhibit a nearly exponential slope and reflect the properties of the collision system at break-up, when the secondary hadrons cease to interact. For example, p_{\perp} spectra of various species measured with lead beam at the SPS have been used to establish collective flow of hadrons and freeze-out temperatures in heavy-ion collisions. In pp collisions the spectra develop a power-law-like tail at much higher p_{\perp} which can be described quantitatively (above about 4 GeV/c) by hard scattering of partons in the initial phase of the reaction [1–3]. In collisions of nuclei this hard scattering contribution may be strongly modified by partonic energy loss in a deconfined medium [4,2]. The p_{\perp} -region from 1 to 4 GeV/c, often referred to as semi-hard region, is less easy to interpret. Hard processes begin to contribute in this region and compete with low p_{\perp} phenomena. Additionally, in reactions involving nuclei, the spectra are modified in the nuclear environment by partons or hadrons scattering more than once [5–7]. This was realized by Cronin et al. [8] at FNAL in the late 70's when in proton-induced reactions with nuclear targets an enhanced production of high p_{\perp} particles was found compared to a naive extrapolation from pp collisions. Later a similar increase was found in interactions of α -particles at the ISR [10] and also in heavy-ion collisions

with oxygen and sulfur beam at the CERN SPS [11]. If the hypothesis of a high level of rescattering, prerequisite for thermalization, is correct, the slope of p_{\perp} distributions in the semi-hard region could reflect the temperature and expansion dynamics of the system.

In 1995 the CERES (ChErenkov Ring Electron Spectrometer) experiment has taken a data sample of $8 \cdot 10^6$ Pb-Au collisions at the CERN SPS at a beam energy of 158 AGeV/c. The sample covers the most central 35% of 6230 mb geometrical cross section. In this letter, we present charged-pion transverse momentum spectra derived from $2 \cdot 10^6$ pions identified in the range from 1 to 4 GeV/c and near mid-rapidity ($2.1 < y < 2.6$). These data and a preliminary report on hadron spectra has been presented at QM97 [15]. Data on charged-hadron spectra at lower transverse momenta will be published separately [16].

A detailed description of the spectrometer is given in reference [14]. Here we will restrict the discussion of the experimental setup to aspects essential for the present analysis. CERES has been designed to measure electron pairs in ultra-relativistic heavy-ion collisions. Two RICH detectors, with full azimuthal coverage, located before and after a superconducting double solenoid constitute the heart of the experiment. The magnet system deflects each track in azimuthal direction, but maintains the polar. Precise tracking is provided by two silicon drift detectors (SDD) positioned on average 10 cm and 11.5 cm downstream of the target in front of the first RICH and a pad chamber (PC) downstream of the second RICH. The two SDDs also determine the position of the event vertex and measure the charged-particle density $dN_{\text{ch}}/d\eta$. By choosing CH_4 as the radiator gas for the RICH detectors the Cherenkov threshold is high enough ($\gamma_{\text{th}} \approx 32$) to suppress signals from the bulk of hadrons. However, charged pions above 5 GeV/c momentum radiate enough Cherenkov light to be observed in the RICH detectors. The clean environment necessary to detect electrons among hundreds of hadrons is ideally suited for a high-statistics study of those pions which exceed the Cherenkov threshold. Pion identification and momentum measurement are provided via the ring radius measured in the RICH detectors. The azimuthal deflection in the magnetic field gives charge information and redundant momentum determination according to $\Delta\phi = 144 \text{ mrad}/p(\text{GeV}/c)$.

The analysis proceeds in several steps. In the first step pion candidates are reconstructed. Each charged particle track originating from the vertex and traversing the two SDDs is extrapolated downstream to the Pad Chamber. If a Pad Chamber signal is found in a window of 6 mrad in polar and 50 mrad in azimuthal direction (corresponding to a lower momentum cut of 2 GeV/c) ring images are searched for in both RICH detectors at the corresponding locations. Several constraints are imposed to identify a pion track: (i) the two ring images match in radius within 10%, (ii) the radii correspond to the azimuthal deflection in the field within two sigma of the resolution, and (iii) the polar angle coincides within two sigma of the measured resolution in all detectors. Tight cuts on using these constraints remove most false tracks from the sample.

Fig. 1 depicts the correlation of ring radius and azimuthal deflection for all the reconstructed pion candidates after applying the cuts (i) and (iii). Two well-defined regions, corresponding to pions of negative and positive charge, cluster around the expected correlation (dotted line) and clearly stand out above a low level of remaining background tracks.

Nearly all remaining background tracks in the candidate sample can be associated with electron tracks. Two classes of background tracks must be distinguished: (i) physical background of high-momentum electrons and (ii) unphysical background originating from uncorrelated electron rings accidentally matching the track in both RICH detectors. High momentum electrons are easily identified by the mismatching of ring radius, which always is the asymptotic one, and deflection in the magnetic field. The cut used to remove those tracks is depicted in the figure (solid line). Note that this background was scaled up by a factor of 20 to make it visible in the figure. The electron background in the remaining sample was determined using a Monte-Carlo simulation and was found to be negligible at all momenta. The unphysical combinatorial background was measured using an event-mixing technique and subtracted from the data. The low level of this background may be judged from the amount of tracks in Fig. 1 with uncorrelated radius and deflection. The signal-to-background ratio is 100 at a p_{\perp} of 1 GeV/c, and decreases to 10 above 4 GeV/c. At the highest p_{\perp} the background subtraction introduces a systematic error of less than 5%. Kaons are only reconstructed if their momentum is above 20 GeV/c, thus kaon background is suppressed by four order of magnitude at all p_{\perp} .

The momentum can be calculated from the azimuthal deflection and the ring radius, both scales are shown in Fig. 1. In our analysis we use the momentum based on the ring radius which has a resolution of $\Delta p/p \sim 0.0008 \cdot p^2(\text{GeV}/c)^2$, significantly better in the range from 4.5 to 30 GeV/c than the resolution $\Delta p/p \sim 0.035 \cdot p(\text{GeV}/c)$ obtained from the deflection in the magnetic field. The comparison of both momentum measurements fixes the absolute momentum scale to better than 0.5%.

In the last step of the analysis the measured transverse momentum spectrum is corrected for the spectrometer characteristics, the limitations of the reconstruction algorithm, as well as all cuts on the data. All corrections are calculated simultaneously in a Monte-Carlo simulation. Pions, generated with realistic kinematical distributions, were traced through a detailed GEANT [17] implementation of the CERES spectrometer. The pion tracks, subjected to the simulated response of the detector, are embedded in real events and passed through the full analysis chain. The ratio R of Monte-Carlo input to output p_{\perp} distributions is shown in Fig. 2. The fit to the ratio (as shown in Fig. 2) is used to correct the data.

The correction function can be split into three regions. Below p_{\perp} of 1.3 GeV/c the correction increases rapidly as pions fall below the Cherenkov threshold. Expressed in p_{\perp} , the threshold depends on the polar angle and hence the cut-off in Fig. 2 is gradual. The plateau region up to 3 GeV/c reflects the reconstruction efficiency of about 20% including all losses due to analysis cuts. Above the Cherenkov threshold the number of photons and the ring radius steadily increase towards their asymptotic values. Both yield an increase of the reconstruction efficiency and the ring center resolution with increasing momentum, which results in a gradual reduction of the correction towards higher momenta. Above 3 GeV/c the correction factor decreases more rapidly due to the deterioration of the momentum resolution which artificially increases the apparent yield at high momenta. The systematic uncertainty in the region from 1.5 to 3 GeV/c is less than 10%, below 1.5 GeV/c the error increases slightly up to 15% at 1.2 GeV/c. The correction for momentum smearing generates uncertainties up to 40% at 4 GeV/c. The absolute normalization introduces an additional overall systematic error of 20% independent of p_{\perp} .

Fig. 2 shows the correction function for the full data set, corresponding to the upper 35% of the geometrical cross section. To study the centrality dependence the data were split into 7 exclusive multiplicity bins, covering the range from $dN_{ch}/d\eta$ of 100 to about 400. For each bin the correction was calculated separately to take into account the reduction of the reconstruction efficiency and the deterioration of the momentum resolution with event multiplicity. The absolute value of the correction function increases by a factor of 2 from the lowest to the highest multiplicity events. No change of the p_{\perp} dependence of the correction was observed.

The final p_{\perp} spectrum is shown in Fig. 3. Since π^+ and π^- spectra are very similar (see the discussion below) we have averaged positively and negatively charged pions in order to cover the largest possible p_{\perp} range. The open symbols represent the full data sample with an average charged-particle density of 220 corresponding to the upper 35% of the geometrical cross section. The full symbols give the result for a more central event selection, with $dN_{ch}/d\eta = 310$ or about 8% of the geometrical cross section. Our result is in good agreement with the recently measured π^0 spectrum in Pb-Pb collisions at the same energy and similar rapidity [18].

Except for the increase in the yield proportional to the charged particle density both spectra shown in Fig. 3 are indistinguishable. The spectra are exponential over the full range observed. Fitting an exponential function $Ae^{(-p_{\perp}c/T)}$ to the full data sample in the range 1.5 to 3.5 GeV gives an inverse slope parameter $T = 245 \pm 5$ MeV/c. The fit of the $m_{\perp} - m_0$ distribution gives within 1 MeV the same inverse slope parameter. The inverse slope varies by less than 10 MeV locally over the full p_{\perp} range. Note that the slope parameter is significantly larger than the values of about 180 MeV which have been observed at lower p_{\perp} [15].

We have split the data sample into 7 exclusive multiplicity bins. The inverse slope parameter T extracted from each of these bins is plotted in Fig. 4 versus the average $dN_{ch}/d\eta$ of the bin. Over the measured centrality range the inverse slope increases by 7 MeV, which is about 2.4% of its absolute value. The statistical errors are smaller than 1 MeV. The systematic error is 5 MeV (indicated by the brackets in Fig. 4) nearly independent of centrality, thus it is an error on the absolute value but not on the trend of the slope with centrality.

From Fig. 1 it is evident that π^+ and π^- can be measured separately. We have determined the π^-/π^+ ratio for 15 exclusive ring radius bands. The average momentum corresponding to each radius bin is determined using the CERES Monte-Carlo simulation. In particular for large p_{\perp} , this momentum is smaller than calculated from the average ring radius because low momentum pions shift to apparently larger momentum due to the limited resolution. As discussed previously, the inclusive p_{\perp} spectra were corrected for the effect of the momentum resolution. While the systematic errors introduced by this correction are acceptable for the inclusive spectra up to 4 GeV/c, they exclude a meaningful comparison of π^- to π^+ above 2.2 GeV/c. The transverse momentum dependence of the π^-/π^+ ratio is shown in Fig.5. The π^-/π^+ ratio is constant within errors over the entire observed range at a value of 1.028 ± 0.005 , assuming that the systematic errors cancel in the ratio.

The p_{\perp} spectra of charged pions are nearly exponential over more than four orders of

magnitude from 1 to 4 GeV/c in p_{\perp} . This suggests a statistical interpretation of the data. Of course, the inverse slope of about 245 MeV, well above the Hagedorn temperature of 160 MeV [20], can not be interpreted as temperature of a dense system of hadronic resonances. This could point towards early thermalization in a partonic phase. On the other hand, collective transverse expansion, well established by observing a linear increase of the inverse slope with particle mass at lower transverse momenta, might sufficiently increase the inverse slope even at the large p_{\perp} observed in this experiment. Data on π° production at similar p_{\perp} have been interpreted accordingly [18].

Models with initial state scattering on the hadron or parton level [5,6] can explain the momentum spectra for central collisions [15,2]. However, such “random walk” models lead to a much larger centrality dependence of the slope and can be excluded [19]. Wang has shown [2] that perturbative QCD calculation modeling the Cronin effect by p_{\perp} broadening can explain π° data down to 1 GeV/c, and one wonders why they do not seem to reflect any parton energy loss in the hot and dense medium. However, the results depend sensitively on the model of the Cronin effect [21]. One might speculate that the number of consecutive parton scattering processes will increase as the impact parameter decreases.

The π^{-}/π^{+} ratio, which reflects the isospin asymmetry in the final state, is different for statistical and perturbative QCD based models. Perturbative QCD predicts a π^{-}/π^{+} ratio increasing with p_{\perp} and saturating at 1.14, which corresponds to the initial isospin unbalance of the valence quarks. The constant ratio at a much lower level observed in the experiment indicates that below 2.2 GeV/c hard scattering does not dominate. A statistical model which evenly distributes the initial isospin unbalance over all particles in the final state gives a ratio of about 1.06. A more sophisticated analysis, including the effects of hadron decays in the final state [22], results in ratio of 1.05. It increases below 400 MeV/c p_{\perp} but remains fairly constant at larger p_{\perp} .

It remains ambiguous whether a statistical or a perturbative QCD interpretation of the data is more appropriate. Additional information might arise from the observation of angular correlations between high momentum pions.

We are grateful for the financial support by the MINERVA Foundation and the Benozziyo High Energy Research Center.

REFERENCES

1. J.F. Owens et al., Phys. Rev. D18 (1978) 1501.
2. X.N. Wang, Phys. Rev. Lett. 81 (1998) 2655.
3. R. Baier et al., Nucl. Phys. B483 (1997) 291
4. M. Gyulassy and X.N. Wang, Nucl. Phys. B420 (1994) 583; X.N. Wang, M. Gyulassy and M. Plümer, Phys. Rev. D52 (1995) 3436.
5. G.R. Farrar, Phys. Lett. 56B (1975) 185; J.H. Kühn, Phys. Rev. D 13 (1976) 2948; P.M. Fishbane et al., Phys Rev D (1977) 122; M. Lev and B. Petersson, Z. Phys. C21 (1983) 155.
6. A. Leonidov, M. Nardi, H. Satz, Nucl. Phys. A610 (1996) 124c.
7. F. Becattini, Proceedings XXIX Int. Symp. on QCD and Multiparticle Production, Brown University, Providence (RI) August 1999 (World Scientific, Singapur, 2000), in print.

8. D. Antreasyan et al., Phys. Rev. D19 (1979) 764.
9. X.N. Wang, Phys.Rep. 280, (1997) 287.
10. M.A. Faessler, Phys. Rep. 88 (1982).
11. T. Akesson et al., Z. Phys. C 46 (1990) 361.
12. N. Xu et al.(NA44 Collaboration), Nucl.Phys. A610 (1996) 175c.
13. G. Roland et al. (NA49 Collaboration), Nucl. Phys. A638 (1998) 91c.
14. G. Agakichiev et al., Nucl. Instr. Meth. A371 (1996) 16.
15. F. Ceretto et al. (CERES Collaboration), Nucl. Phys. A638 (1998) 467c; Doctoral Thesis F. Ceretto, University of Heidelberg (1998).
16. CERES Collaboration, to be published
17. R. Brun et al. CERN DD/EE/84-1
18. M.M.Aggarwal et al., Phys. Rev. Lett. 81 (1998) 4087.
19. P. Braun-Munzinger and J. Stachel, Nucl. Phys. A638 (1998) 3c.
20. R.Hagedorn, Supp.Nuovo Cimento 3 (1965) 147, Nucl. Phys. B24 (1970) 93
21. M. Gyulassy, P. Levai, Phys. Lett. B442 (1998) 1.
22. P. Braun-Munzinger, I. Heppe, J. Stachel, Phys.Lett. B465 (1999) 15; I. Heppe, Diploma These, University of Heidelberg, 1998.

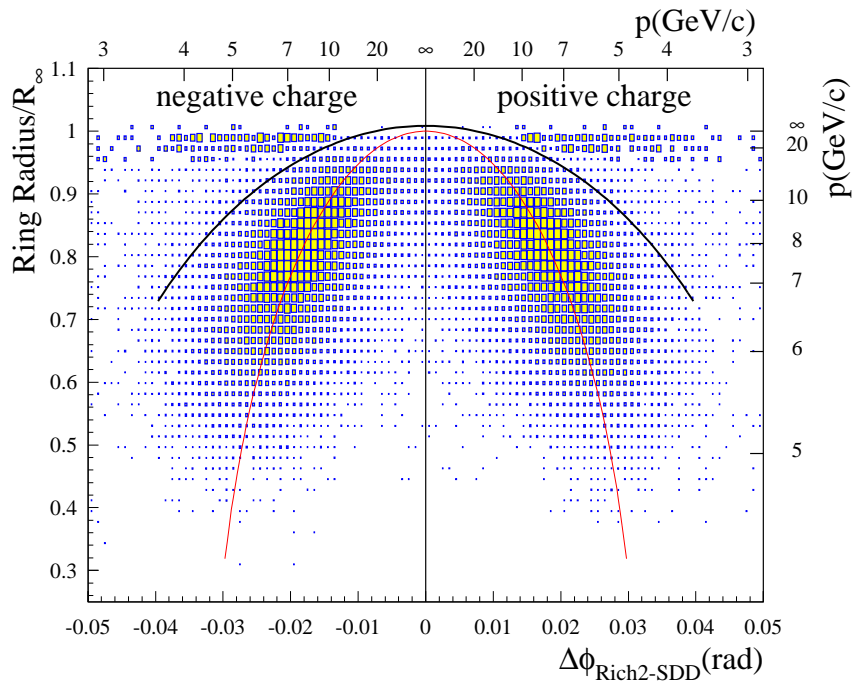


Figure 1. Correlation between Cherenkov ring radius (in units of the asymptotic ring radius R_∞) and azimuthal deflection in the magnetic field for reconstructed positive and negative pions. The top and right side of the figure indicate the corresponding momentum scales derived from both quantities. The dotted line shows the correlation expected for pions. The solid line represents the cut used to suppress electron tracks which survive the two sigma cut on the match between radius and phi deflection. In order to illustrate the cut and to visualize this background, which is at a very low level, all entries above R/R_∞ of 0.95 have been multiplied by a factor of 20.

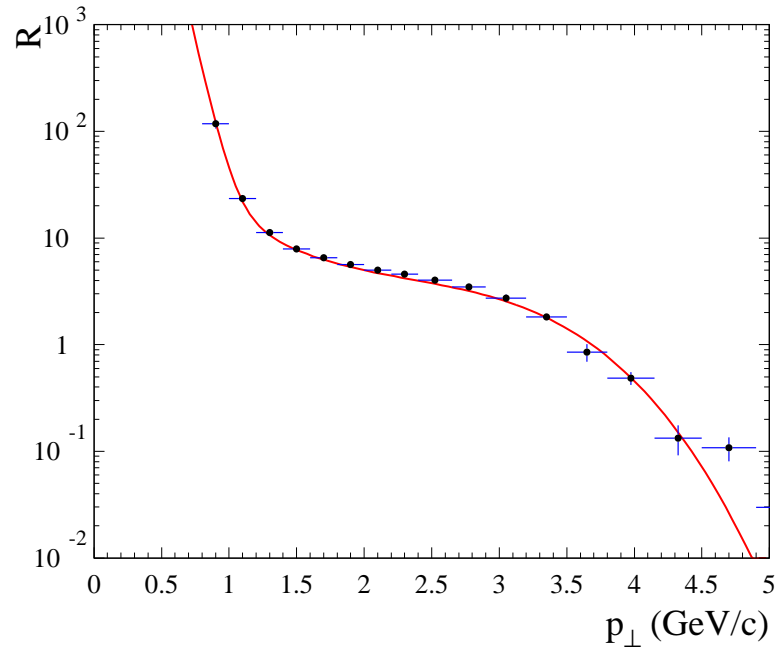


Figure 2. Correction function used to correct the pion p_{\perp} distribution obtained for the full data set. The function is determined iteratively from a Monte Carlo simulation as ratio of input distribution to the one reconstructed through the full analysis chain. The function corrects for limited reconstruction efficiency, all analysis cuts, acceptance and resolution of the spectrometer.

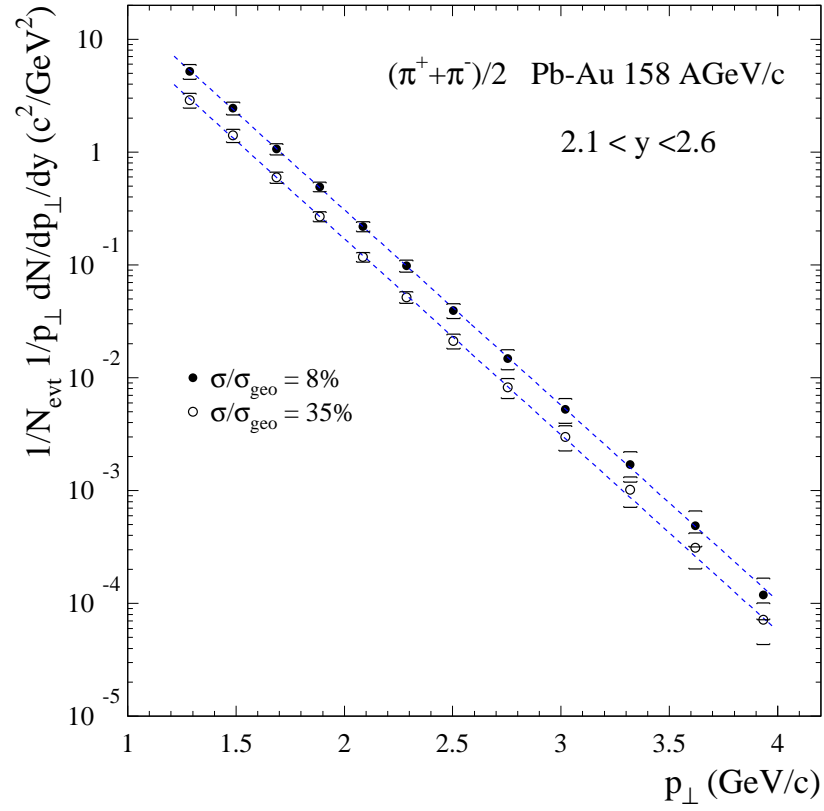


Figure 3. Invariant transverse momentum distribution of positively and negatively charged pions. Shown are the distributions for the full data sample and for the most central fraction of the data, corresponding to 35% and 8% of the geometrical cross section, respectively. The lines are exponential fits to the data.

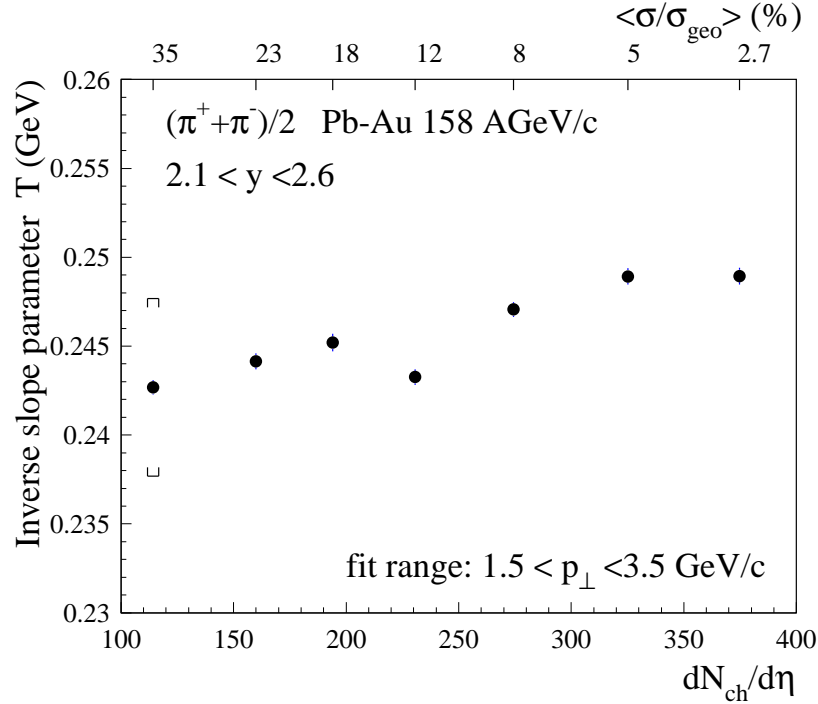


Figure 4. Centrality dependence of the inverse slope parameter T . The slope parameter is extracted from fitting an exponential function to the invariant p_{\perp} distribution obtained from exclusive event samples. The abscissa shows the average charged particle density of each event sample. The scale at the top gives the fraction of the geometrical cross section integrated above the corresponding charged particle density. Error bars represent statistical errors, the bracket indicates the systematic error.

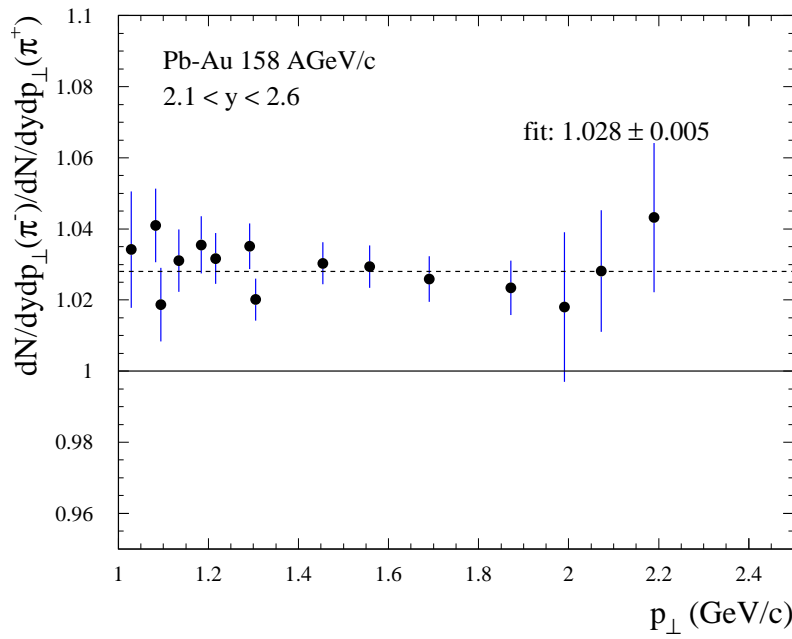


Figure 5. Transverse momentum dependence of the π^{-}/π^{+} ratio.